Influence of Environment on Proton-Transfer Mechanisms in Model Triads from Theoretical Calculations

G.-S. LI, B. MAIGRET, D. RINALDI, M. F. RUIZ-LÓPEZ

Laboratoire de Chimie théorique, Unité Mixte de Recherche CNRS-UHP, No. 7565 (Institut Nancéien de Chimie Moléculaire), Université Henri Poincaré, Nancy I, BP 239, 54506 Vandoeuvre-lès-Nancy Cedex, France

Received 10 January 1998; accepted 30 May 1998

ABSTRACT: We have carried out theoretical calculations to analyze molecular interactions and proton transfer mechanisms in the formate–imidazole–water system, which may be considered the simplest model of catalytic triads in serine proteases. Computations were carried out at the density functional theory level. The effect of a dielectric environment on energy surfaces is considered using a polarizable continuum model and the self-consistent reaction field approach. The role played by inertial and noninertial polarization of this environment is emphasized. Nonequilibrium solvation effects have been estimated. The results show that there are different reaction mechanisms, concerted or stepwise, that may be competitive, depending on the nature of the molecular environment.
 J Comput Chem 19: 1675–1688, 1998

Introduction

Serine proteases catalyze the hydrolysis of peptide bonds and therefore play a major role in the metabolism of animals. The hydrolysis mechanism has been the subject of a great deal of attention both from experimental[1–10] and theoretical[11–20] points of view. Basically, serine proteases have an active center that consists of a catalytic triad built-up from aspartic acid, histidine, and serine residues. Histidine contains an imidazole ring that exhibits striking chemical properties because it can behave either as proton donor or proton acceptor. This double functionality is certainly of fundamental importance for explaining the enzymatic activity of serine proteases, but, in spite of the considerable work devoted to the elucidation of the catalytic mechanism,[1–20] several questions remain unanswered. A charge relay mechanism was first proposed by Blow et al.[2a] and modified later by Hunkapiller et al.[2b] According to these works, the catalytic reaction mechanism involves a double proton transfer from Ser to His and from His to the Asp residue, with formation of

Correspondence to: M. F. Ruiz-López

CCC 0192-8651 / 98 / 151675-14

the high nucleophilic species, $SerO^-$ which may in this way attack the substrate (see Fig. 1a). There are some experimental data supporting this mechanism[2,21] as well as experimental evidence against it.[3,22] An alternative mechanism[1] assumes that there is no proton transfer from His to Asp, the carboxylate of Asp stabilizing the forming imidazolium cation (see Fig. 1b). Other investigators suggest that the role of Asp is also to fix the tautomeric form of the imidazole ring and to anchor His in the correct orientation.[3c] Catalytic triads are present in other enzymes as well.[23]

A number of theoretical calculations on model systems are available. Earliest computations at the semiempirical level showed the double proton transfer in the catalytic triad to be favorable[11,12] although more recent PM3 computations[17] are consistent with single-proton-transfer mechanisms. *Ab initio* calculations[13] have also predicted that the Asp^- His^+ Ser^- structure is more stable than the Asp^0 His^0 Ser^- one. These previous works have considered gas-phase processes and the conclusions reached for the mechanism cannot be extrapolated to enzymatic reactions. Indeed, some investigators demonstrated that the role of the environment is crucial.[14,15] Longo et al.[14d] carried out semiempirical computations on a model of α-chymotrypsin. The environment was modeled by the electric field generated by the electrostatic charges at the polarizable protein backbone, the structure of which was derived from crystallographic data. The multicharged structure Asp^- His^+ Ser^- appeared to be the most sensitive system toward surrounding effects. A detailed empirical valence bond (EVB) approach was carried out by Warshel and Russel[15a] to investigate the catalytic activity of trypsin. The analysis indicated that the main factor in the catalytic mechanisms is the stabilization of the tetrahedral intermediate by the N—H dipoles of the oxyanion hole and by bound water molecules. Moreover, free-energy computations allowed these investigators to conclude that the charge relay mechanism is unlikely to be important because it involves a larger free energy barrier (10 kcal/mol). Warshel et al.[15b] confirmed these conclusions through thermodynamic analysis based on the use of p*Ka*s in solution together with computations for the enzyme. One must finally note, for completeness, that the role of water molecules has been discussed through molecular dynamics (MD) simulations[18] and by *ab initio* computations[20a] that focused on the catalytic role of a water molecule in one-step serine protease acylation processes.

Connected with the problem of the mechanism of serine proteases, there has been, in recent years, discussion on the exact role of low-barrier hydrogen bonds (LBHB).[10,24] Formation of such bonds (for a unique definition see ref. 241) has been postulated to contribute to enzymatic catalysis by supplying 10–20 kcal/mol and facilitating difficult reactions.[10a,24d] This effect would arise when the p*Ka* values of the atoms sharing the hydrogen atom become similar, although some experiments

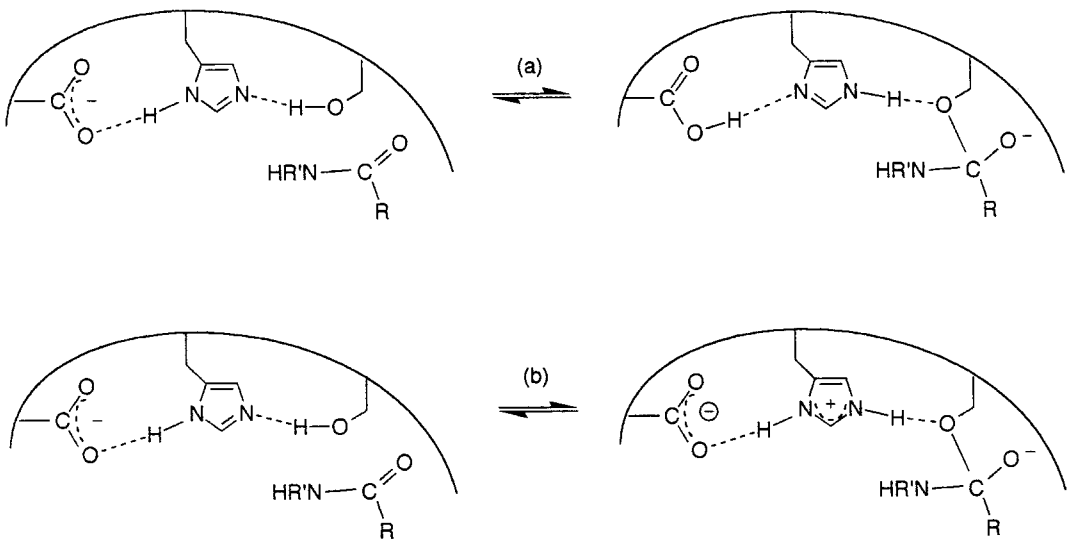

FIGURE 1. Schematic representation of serine protease catalytic mechanism: (a) charge relay mechanism; and (b) single proton-transfer mechanism.

do not support this.[24j] *Ab initio* calculations for model systems in the gas phase have shown that LBHB may indeed furnish 20 kcal/mol more than normal hydrogen bonds,[24m] but p*Ka* equalization does not appear to be the main condition for LBHB formation — energy degeneration of the two minima in a short hydrogen bond being a possible origin for that.[24n] The role of LBHB in enzymatic catalysis has been criticized[24g] because environmental effect tends to destabilize the transition state, in which the charge is delocalized, relative to the asymmetric minima, in which the charge is localized, and thus LBHB may lead to anticatalysis.

Some other theoretical studies have been reported in which combined quantum mechanics and molecular mechanics computations have been employed.[25]

A better understanding of molecular interactions within the constituents of catalytic triads appears to be an important goal for acquiring deeper insight into the associated enzymatic reaction mechanisms. In the present study, we investigate the interactions and proton transfer mechanisms within a simple model, namely, an imidazole molecule interacting with a formate anion and with a water molecule, using density functional theory calculations. The choice of the system has been made on the basis of the available computational capabilities. The effect of substituting hydrogen atoms by other groups is briefly commented upon, but it has not been possible to carry out computations in that case. Semiempirical approaches could be used for that purpose, but, as usual in such studies, *ab initio* computations for model systems are necessary to calibrate the results. We describe in detail the interactions within the system assumed to be either isolated (gas phase) or placed in a dielectric medium. Our objective is to obtain insight into the environment effects on the potential energy surface (PES) corresponding to proton transfer processes in the system and to discuss the factors that favor or disfavor the proton relay mechanism.

Although our model is quite simple, the use of specific geometric constraints allows one to account for actual residue arrangements in enzymes. For instance, the common arrangement of Asp, His, and Ser in catalytic triads is so that the distance between (Asp)O $\cdots$ N(Im) atoms is estimated to be not far from 2.8 Å, whereas the (Ser)O $\cdots$ N(Im) distance is about 3.0 Å.[2a,4] During the reaction, these distances may change only within a restricted range because of enzyme constraints. On the other hand, it is well-known that the shape of the PES for proton transfer is quite dependent on the proton-donor atoms distance and that fixing this distance may lead to results substantially different from those that would be obtained though full geometry optimization. Considering these points, computations have been carried out assuming fixed values of the ON lengths and analysis of the effect of these values on the final results. The same strategy has often been used in theoretical calculations with model systems.[17,18,24g,24h,24i]

We have also examined the role of fluctuations of the environment, which is important for understanding proton-transfer dynamics both in solution[26] and enzymatic reactions.[27] In the present study we simply consider the role of a fluctuating electric field in the case of a model system in aqueous solution. The enzyme electrostatic potential fluctuations have been found to be a key dynamic factor in reactions that involve large charge rearrangement,[27] although one must keep in mind that fluctuations may be unimportant in regard to enzyme catalytic effect, taken as the difference in energetics of a given reaction at the active enzyme site and in solution, because dynamics effects in enzyme and solution environments may be similar.[26a,27]

Method of Calculation

Calculations were carried out using the density functional theory (DFT) approach. There are several reasons for this choice. First, the use of accurate correlated *ab initio* calculations would be too costly, considering the number and size of the systems investigated. Besides, the present computations are intended to serve as a reference work for future studies using combined density functional and molecular mechanics approaches, which have been recently implemented to study the dynamics of chemical reactions in solution.[26c] Moreover, DFT has been shown to describe hydrogen-bond interactions reasonably well, provided that gradient-corrected functionals are employed.[28]

The Becke–Lee—Yang–Parr (BLYP) functional has been used here. The exchange functional consists is a Slater functional modified by a density-gradient term.[29] The correlation functional also contains density-gradient corrections.[30] The basis set used is 6-31G*.[31] This computational level is noted BLYP/6-31G*.

The effect of a dielectric environment has been taken into account through the use of a self-consistent-reaction-field (SCRF) method. We assume that the system is surrounded by a polarizable continuum with relative dielectric permittivity equal to that of water (80.0). The Hamiltonian of the system includes the corresponding interactions with the continuum, which are computed through a multipole expansion of the reaction potential. The method is well documented in the literature[32] and will not be further described.

The calculations were carried out using Gaussian-94[33] and an updated version of SCRFPAC.[34] The molecular geometries were optimized, although some constraints were imposed. The SCRFPAC algorithm permits full or partial geometry optimization of solvated systems in a very efficient manner. In all cases, the system was assumed to be planar and the hydrogen bonds assumed to be linear. The ON distances (O belonging to either formate or water) were fixed unless otherwise noted. The choice of the ON bondlengths was made after analysis of x-ray structures of several enzymes.[2a,4]

The potential energy surface (PES) for proton transfer was estimated, in some cases, through a scan of the proton position. This allows investigation of some qualitative trends for energy barriers. In the case of proton transfer in model triads, transition structures were determined rigorously using the Berny algorithm[35] (except for the double-proton-transfer mechanism; see subsequent text).

Structure of Model System $HCOO^-$–Imidazole in Gas Phase and Polar Dielectric Environments

We first consider the formate–imidazole system (I). This complex yields, through proton transfer, the formic acid–deprotonated imidazole complex (II), as represented in Scheme I.

The relative stability of the two complexes depends on proton affinity of the two anions. The computed quantities for $HCOO^-$ and Im^- are 355.7 and 360.0 kcal/mol, respectively. Although these values are larger than the experimental quantities, 347.636 and 350.2 kcal/mol,[37] respectively, the calculations correctly predict the larger proton affinity of Im^-, with the computed difference (4.2 kcal/mol) being not far from experiment (2.6 kcal/mol). Note that the accurate computation

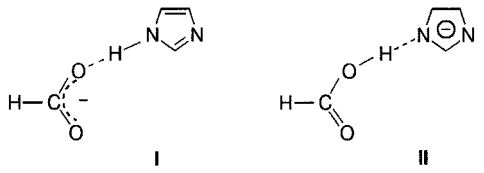

I II

SCHEME 1

of absolute proton affinities usually requires using extended basis sets and high-level correlated methods, as we have shown before for methylimidazole.[38] The previous results suggest that, in the computations that follow, the imidazole ring deprotonation energy will be slightly overestimated.

When the imidazole–formate complex is fully optimized in the gas phase (although maintaining the planarity of the system and the linearity of the hydrogen bond), one energy minimum is found corresponding to complex I. Full optimization starting from a molecular geometry corresponding to complex II leads to complex I. In other words, there is no energy minimum in the adiabatic curve corresponding to complex II. The optimized ON and NH distances for complex I are 2.714 Å and 1.083 Å, respectively. Note that two possible conformations of formate are possible, although in this work we only give the results for the most stable one, which is that schematized in Scheme I.

To take account of geometrical constraints in the structure of the catalytic triad, further geometry optimizations of the complex have been carried out by keeping the ON bondlength constant. Because this bondlength is estimated to be close to 2.8 Å in the catalytic triads,[2a,4] we have carried out a series of computations for different values of this distance, namely, 2.6, 2.8, and 3.0 Å. Table I contains the optimized values of NH and OH distances for each value of ON. Note that, for the ON distance of 2.6 Å, as has happened for the fully optimized distance, a single minimum of type I is obtained. However, for larger ON distances, minima are predicted for structures of types I and II. In these cases, the formate–imidazole complex I is more stable than complex II.

The NH bondlength in isolated imidazole at this level of calculation is 1.018 Å. Therefore, when imidazole is interacting with formate, the NH bond is lengthened by an amount that depends on the ON bondlength. The shorter the ON bondlength, the larger the NH one. Similar constraints hold for the OH bond in II (OH is 0.989 Å in isolated formic acid).

TABLE I.

Computed Values for NH and OH Interatomic Distances (Å) and Solvation and Relative Energies (kcal / mol) for Complexes Formate–Imidazole (I) and Formic Acid–Imidazolate (II) at Fixed Distances Between Imidazole N and Formate O Atoms.

	I		II		
	ΔG^{sol}	d_{NH}	ΔG^{sol}	d_{OH}	$E_{II} - E_I$
d_{ON} = 2.6 Å					
Gas phase		1.0942			
Aqueous solution (a)	−52.5	1.0942	No energy minima		
Aqueous solution (b)	−52.6	1.0830			
d_{ON} = 2.8 Å					
Gas phase		1.076		1.109	9.6
Aqueous solution (a)	−52.3	1.076	−53.5	1.109	8.3
Aqueous solution (b)	−52.5	1.065	−53.7	1.073	
d_{ON} = 3.0 Å					
Gas phase		1.062		1.063	11.7
Aqueous solution (a)	−52.8	1.062	−54.6	1.063	9.9
Aqueous solution (b)	−53.1	1.053	−54.9	1.042	

[a] Optimized geometry in the gas phase.
[b] Optimized geometry in solution.

Table I summarizes the results obtained for geometry optimization in a polar dielectric surrounding. These dielectric effects give an idea of how a polar environment will modify Asp–His interactions. In such a medium, the electrostatic effect decreases slightly the energy difference between I and II, because it stabilizes preferentially the formic acid–deprotonated imidazole complex II by 1–2 kcal/mol.

The most relevant effect of dielectric surrounding is shortening of AH bonds, A being the donating atom. In other words, electrostatic interactions disfavor proton donation. This effect contrasts with the solvent cooperativity phenomenon reported for the imidazole–water molecule complex in water solution, which makes the hydrogen bond stronger and favors proton transfer.[38b] The opposite environment effect observed here is explained by the fact that the hydrogen bond links a neutral proton-donating group to a charged base. The dielectric environment always favors charge concentration and this is achieved by decreasing of AH bondlengths, which minimizes intermolecular electronic charge transfer. Note also that the solvation energy is increased very slightly by the effect of geometry relaxation in the dielectric.

It is instructive to compare these results with qualitative predictions based on the use of experimental p*Ka* values for imidazole and HCOOH (roughly 15 and 4, respectively). Thus, if one considers the process $AH + B^- \rightarrow A^- + BH$, the free energy of the reaction may be estimated from: $\Delta G = 2.303\ RT\ [pKa(AH) - pKa(BH)]$. Replacing AH and BH by imidazole and formic acid, respectively, one finds $\Delta G \approx 15$ kcal/mol. This procedure assumes separated ions, whereas, in our case, we have a complex in which the species have been constrained to lie at a given fixed distance. In principle, it would be possible to estimate an energy correction arising from the electrostatic interaction of the ions within the dielectric,[15b] although such an approach cannot accurately describe the large polarization of the system at short interion distances. Looking at the values in Table I one sees that the energy difference increases with distance (ΔE_{II-I} changes roughly from 8 to 10 kcal/mol when d^1_{ON} changes from 2.8 to 3.0 Å) so that the value predicted using p*Ka*s seems to be consistent with the result of calculations (see also Fig. 2).

A final comment on these calculations is relevant. The evaluation of acid–base equilibria in water is difficult for several reasons. The theoretical model must allow accurate computation of protonation free energies in gas phase as well as accurate solvation energies for the species involved. In previous works, we have analyzed this point in detail in the case of methylimidazole.[38b] We have shown that the cavity model employed

here appears to yield reasonable values for absolute p*Ka*s, provided one uses a sophisticated computational level (in particular very extended basis sets). Therefore, the main source of error in our computations is expected to come from the relatively simple basis set considered (e.g., the errors on absolute gas-phase proton affinity may reach 10 kcal/mol, as previously noted).

Structure of Model System $HCOO^-$–Imidazole–Water in Gas Phase

It is of interest to examine the interactions in the $HCOO^-$–imidazole–water system chosen to model the catalytic triad. Full geometry optimization of structures III and IV represented in Scheme II in gas phase led to a single minimum of type III. The ON distances between formate–imidazole and water–imidazole are 2.676 and 2.891 Å, respectively.

Further geometry optimizations of structures III and IV were carried out by fixing d^1_{ON} (the ON distance between imidazole and formate) to 2.6, 2.8, and 3.0 Å The position of the water molecule is still fully relaxed with the aim of comparing the effect of hydrogen bond to electrostatic solvation effects. In particular, the cooperativity effect due to hydrogen-bond formation of imidazole with water is expected to play an important role.[38b] Proton transfer from water to imidazole at fixed ON distances is examined in what follows.

For the three ON distances, stable structures for both complexes are predicted in gas phase. Results are summarized in Table II. The ON distance between serine and histidine in catalytic triads is close to 3.0 Å,[2a,4] which is not very far from optimized values for the corresponding distance d^2_{ON} between imidazole and water in IV. The optimized d^2_{ON} length decreases when the proton is transferred to formate (i.e., the hydrogen bond with water is strengthened). Indeed, the water molecule in the model triad stabilizes substantially the imidazolate anion. Hence, the energy difference between IV and III (e.g., 6.6 kcal/mol for d^1_{ON} = 2.8 Å) is notably smaller than the corresponding energy difference between II and I in gas phase (9.6 kcal/mol) or in a dielectric environment (8.3 kcal/mol).

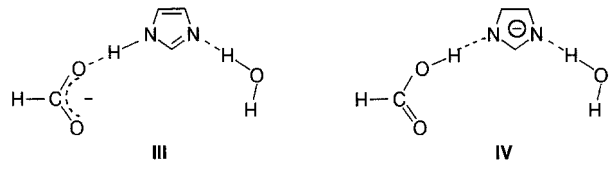

III IV

SCHEME 2

Energy Profiles for Proton Transfer from Imidazole to Formate

Proton transfer from imidazole to formate is now examined. We consider two different cases, proton transfer from I to II and from III to IV. The role of the dielectric environment is also taken into account.

We start the proton transfer process from I to II in both the gas phase and in a polar dielectric medium. The activation energies are estimated as follows. The reaction coordinate is assumed to be defined essentially by the NH distance. Thus, we make a scan of this internal parameter and optimize the other parameters at each step (keeping the planarity of the system and a fixed ON distance as usual). This computation is first carried out in gas phase. In the dielectric continuum, single-point computations are done for gas-phase geometries, because, as seen before, geometry relaxation in aqueous solution leads to small solva-

TABLE II.

Computed Values for Some Interatomic Distances (Å) and Relative Energies (kcal / mol) for Formate–Imidazole–Water (III) and Formic Acid–Imidazolate–Water (IV) Complexes in Gas Phase at Fixed ON Distances.[a]

	III			IV			
d^1_{ON}	d^2_{ON}	d^1_{NH}	d^2_{NH}	d^2_{ON}	d^1_{NH}	d^2_{NH}	ΔE_{IV-III}
2.6	2.888	1.107	1.882	No energy minima			
2.8	2.894	1.082	1.890	2.852	1.711	1.840	6.6
3.0	2.902	1.065	1.899	2.847	1.946	1.832	6.3

[a] d^1_{XY} refers to the formate–imidazole moiety, whereas d^2_{XY} refers to the imidazole–water moiety.

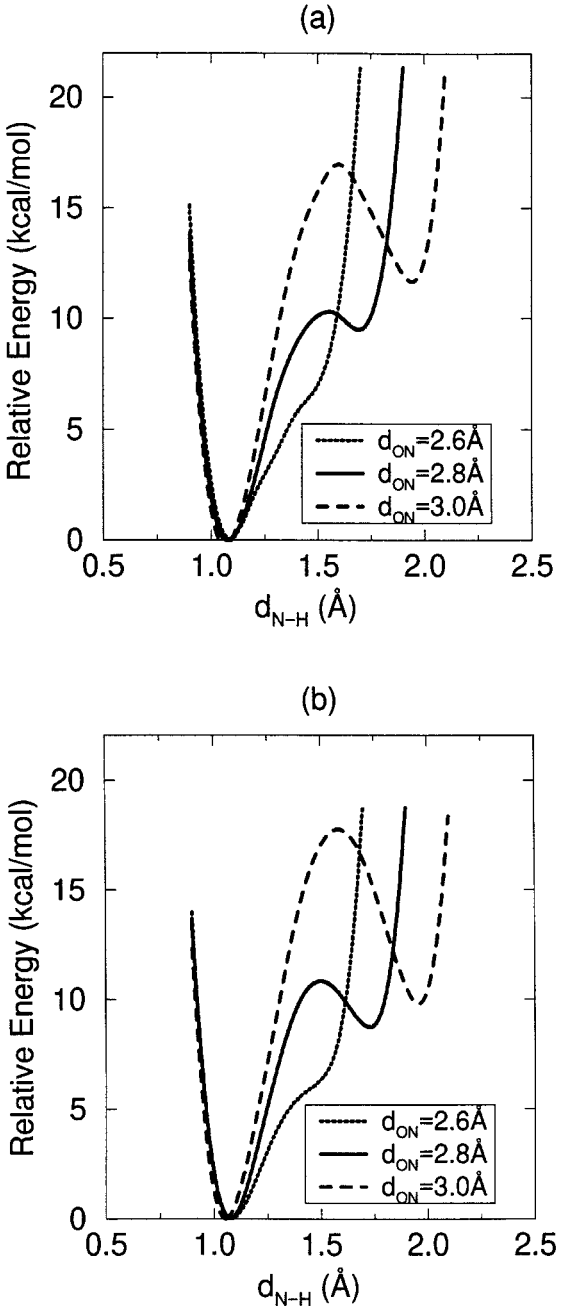

FIGURE 2. Energy profiles for proton transfer from imidazole to formate I → II in gas phase (a) and in aqueous solution (b) for fixed values of ON distance.

tion energy changes (see Table I). The corresponding energy profiles are shown in Figure 2. The activation barriers obtained for d^1_{ON} values 2.8 and 3.0 Å are given in Table III.

The activation barriers for process I → II or II → I increase substantially with d^1_{ON} distance. Also, all barriers increase through electrostatic effect, because the transition structures solvation energies are lower than those for I or II. The reason is again the preferential solvation of charge-localized structures (i.e., the reactant or the product in the present case). So, although thermodynamically the electrostatic effect tends to favor proton transfer (ΔE_{II-I} decreases; see Table I), the process is not favored kinetically. The effect is not very large if one considers a dielectric constant equal to that of water, but it could be more significant in the presence of neighboring ions that would produce a higher electric field.

Activation barriers for process I → II are substantially larger than kT at normal temperature, whereas the reverse process II → I barriers are very slight at an ON distance of 2.8 Å. For distances larger than 2.8 Å proton transfer becomes progressively more difficult, whereas, for shorter distances, there is a single well with an energy minimum of type I. One must keep in mind that the computed proton affinities for $HCOO^-$ and Im^- are overestimated, but the error is larger for the latter. Therefore, the stability of I with respect to II and the corresponding activation barrier for I → II are probably slightly exaggerated.

We now consider the process III → IV; that is, the proton transfer when a water molecule is hydrogen bonded to the N atom of the imidazole ring. The energetics are presented in Table IV and Figure 3. We have already noted that the water molecule stabilizes more the deprotonated imidazole ion than the neutral imidazole molecule, therefore the relative energy is lower for IV—III than for II—I. The stabilization of the transition state is intermediate to the reactant and product stabilization, so the activation barrier for direct proton transfer decreases by the effect of water solvation, whereas it increases for backtransfer. This is somewhat different than the effect due to electrostatic solvation seen previously for the I ↔ II

TABLE III.
Energy Barriers (kcal / mol) for Proton-Transfer Processes at Fixed d^1_{ON} Distances.

	d^1_{ON} = 2.8 Å		d^1_{ON} = 3.0 Å	
	I → II	I ← II	I → II	I ← II
Gas phase	10.2	0.7	16.9	5.2
Aqueous solution (a)	10.5	2.2	18.0	8.1

[a] Optimized geometry in the gas phase.

TABLE IV.
Energy Barriers (kcal / mol) for Proton-Transfer Processes at Fixed d^1_{ON} Distances.

	d^1_{ON} = 2.8 Å		d^1_{ON} = 3.0 Å	
	III → IV	III ← IV	III → IV	III ← IV
Gas phase	8.3	1.7	15.0	7.0
Aqueous solution (a)	9.3	3.2	16.0	9.7

[a] Optimized geometry in the gas phase.

process, which tends to increase activation barriers for both direct and backtransfer. Therefore, it is of interest to consider a hybrid discrete-continuum model that allows to account for both hydrogen bonding (which stabilizes the imidazolate, i.e., favors product stabilization) and long-range interactions (which favors the reactant and product with respect to the transition structure). If one compares the corresponding barriers (see Table IV, results in solution) to the results obtained for I ↔ II in a vacuum (see Table III, results in gas phase), it can be seen that: (1) the direct transfer III → IV is favored with respect to I → II in gas phase; and (2) the backtransfer III ← IV is disfavored with respect to II ← I in gas phase. Therefore, specific interactions may modify the usual idea that, in $AH \cdots B^- \rightarrow A^- \cdots HB$ processes, solvation energy always tends to increase the activation energy barriers. This may arise, for instance, when one of the anions forms strong hydrogen bonds with the solvent and the other does not. Continuum models of the solvent are generally well adapted to evaluate electrostatic solvation energies, but one must be aware of their limitations in reproducing some energy contributions in specific interactions, such as charge transfer, which is clearly important in the case of anion solvation. A more sophisticated model of the solvent should treat at least the first solvation shell discretely (and allow for polarization and charge transfer). In our case, this could be done by including other explicit water molecules in the supermolecule, but obviously the computational cost would increase considerably.

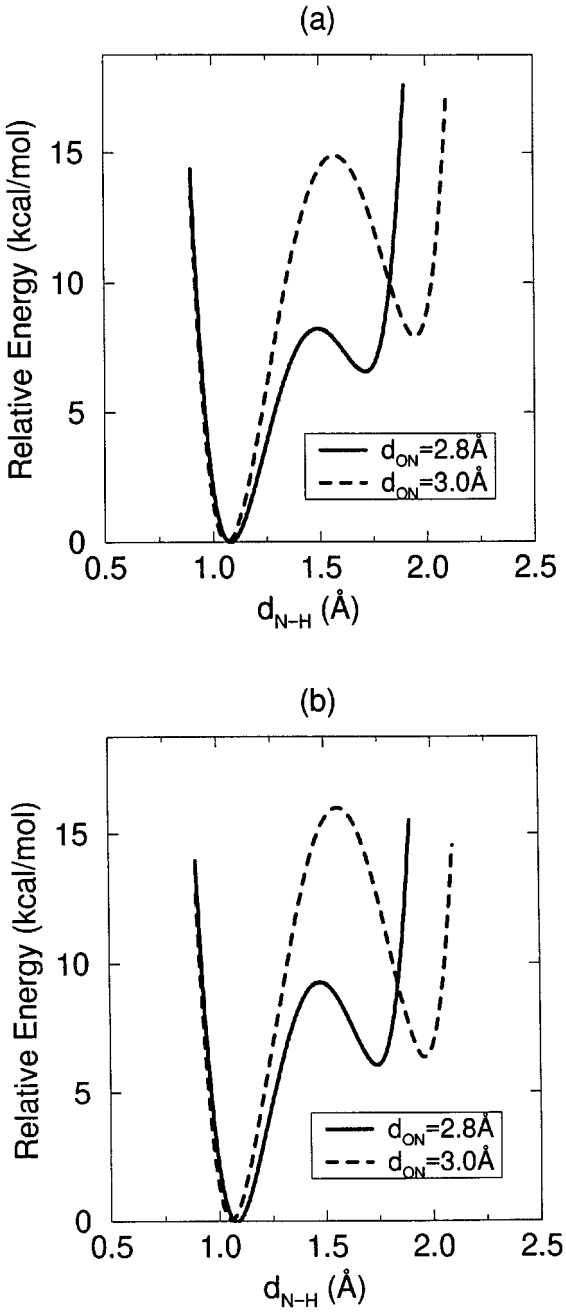

FIGURE 3. Energy profiles for proton transfer from imidazole to formate III → IV in gas phase (a) and in aqueous solution (b) for fixed values of ON distance between formate and imidazole.

Charge Relay versus Single-Proton-Transfer Mechanisms

We now compare the two mechanisms usually considered for catalysis in the Asp–His–Ser triad. The charge-relay mechanism involves a double-proton transfer from Ser to His and from His to Asp (see Fig. 1a). The single-proton-transfer mechanism involves only proton transfer from Ser to His (see Fig. 1b). Investigation of the catalytic mechanism supposes that interaction of the form-

ing $SerO^-$ with the substrate is taken into account. However, in this study, we limit our investigation to the analysis of potential energy surfaces for proton transfer in the model triad. The main objective is to get relative energies for the species involved in the processes, including transition states, in the presence of a polarizable surrounding.

Our model for this study is the formate–imidazole–water system. The entire system is placed in a polar dielectric continuum. Proton transfer from Ser to His is modeled by proton transfer from water to imidazole. To model this reaction, some additional constraints have been imposed during the geometry optimization procedure. The d^1_{ON} and d^2_{ON} distances have been fixed at 2.8 Å and 3.0 Å, respectively (as before, we consider planar systems and linear hydrogen bonds; to accelerate convergence, the imidazole ring is also assumed to be frozen during the chemical process, but this does not seem to be a severe approximation). Four minima are obtained. Structures of type III and IV (see Scheme II) correspond to the reactants in two possible states. Structures V and VI, depicted in Scheme III, correspond to the possible configurations for the products (note that, in gas phase, the latter structures are not energy minima, even with geometrical constraints; the stabilizing role of the dielectric continuum is thus crucial).

The double-proton transfer III → VI is achieved by a charge-relay mechanism, which may be concerted or stepwise. The concerted process (hereafter called mechanism CR1) would proceed through a synchronous transfer of both protons. The stepwise mechanism (hereafter called mechanism CR2) would proceed through a proton transfer from imidazole to formate (III → IV) followed by a transfer from water to imidazole (IV → VI).

The single-proton transfer, on the other hand, is modeled by the process III → V (mechanism SP). Note that conversion between the two possible product species (V ↔ VI) is possible through proton transfer in the formate–imidazole moiety.

The transition structures (TSs) corresponding to all these elemental processes have been localized and some pertinent geometrical parameters are summarized in Table V. Localization of the TSs is provided here using the Berny algorithm;[35] therefore, they are true saddle points in the restricted potential energy surface of the system (i.e., the surface obtained after constraining some internal parameters).

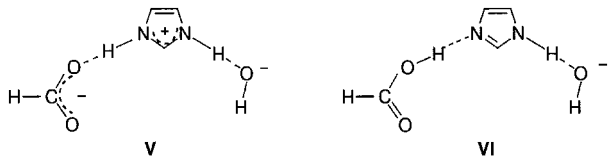

V VI

SCHEME 3

In the case of the concerted CR1 mechanism, III → VI, all TS search computations that we tried converged systematically to the TSs corresponding to single-proton transfers (either III → IV or III → V). This seems to indicate that the concerted double-proton transfer is impossible in this system. However, because we cannot completely exclude the existence of such a TS (in this or related systems) we considered an approximate transition structure, obtained by looking at the maximum energy value that results from a synchronous scan of the two proton coordinates. The relative energies of all the species implicated in the different mechanisms are shown in Figure 4.

Figure 4 shows the concerted CR1 mechanism pass through a TS, which is about 7 kcal/mol higher than the TS for a single-proton transfer mechanism SP. The stepwise mechanism (CR2) presents a first TS for imidazole → formate proton transfer at 9.5 kcal/mol above reactant III, whereas the second TS energy is at least 25.8 kcal/mol above the reactants. Indeed, the relative energy of this TS is very close (below the method accuracy) to the TS corresponding to the single proton mechanism. What can be concluded from these results? The concerted double-proton mechanism can be discarded because it requires higher activation energy. Conversely, the stepwise CR2 and the single-proton SP mechanisms appear to be competitive and we cannot discard one of them on the basis of our computations.

TABLE V.
NH Distances for Reaction Intermediates and Transition Structures in Figure 4 (Å).

System	d^1_{NH}	d^2_{NH}
III (−0 0)	1.067	1.997
IV (0 − 0)	1.739	1.989
V (− + −)	1.094	1.066
VI (0 0 −)	1.767	1.045
TS (III → IV)	1.477	1.992
TS (III → V)	1.080	1.427
TS (III → VI) (a)	1.458	1.442
TS (IV → VI)	1.754	1.500
TS (V → VI)	1.394	1.056

[a] Estimated values using proton scan (see text).

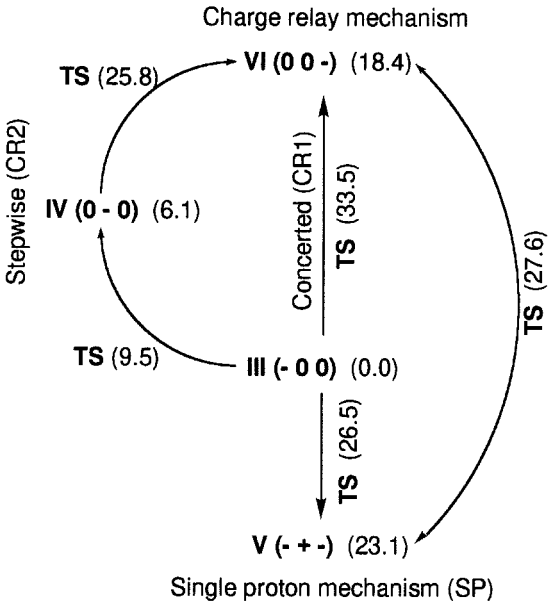

FIGURE 4. Energy diagram for the different proton transfer processes considered. Data in parentheses give the energy (kcal / mol) of the structure relative to reactant III. For clarity, a schematic charge distribution for the energy minimum structures that corresponds to charges on the Asp–His–Ser system is provided. For instance, $(-0,0)$ refers to the formate–imidazole–water system III, whereas $(-+-)$ refers to the formate–imidazolium–hydroxyl system V. The relative energy for the transition structure corresponding to the concerted process has been estimated, as explained in the text.

These results may be compared with previous theoretical computations. For instance, it has been shown through *ab initio* computation for the $NH_3 \cdots$ imidazole $\cdots NH_4^+$ system[39] that concerted double-proton transfer is much less favorable than stepwise processes. The difference in energy between CR1 and SP mechanism (7 kcal/mol in the present case) may be compared with the free energy difference obtained by the empirical valence bond approach carried out by Warshel and Russel[15a] for trypsin (10 kcal/mol). We must emphasize that our computations do not include zero-point energies or temperature corrections that would in any way modify our results for relative energies.

Comparison can also be made with energetic predictions from p*Ka* values, as explained earlier. Using the experimental p*Ka* value for HCOOH (4), imidazol (15), protonated imidazole (7), and water (16), one can deduce the free energy change for the three proton transfer processes examined in Figure 4:

$$HCOO^- + Im \rightarrow HCOOH + Im^- \qquad \Delta G = 15.0 \text{ kcal/mol}$$

$$Im^- + H_2O \rightarrow Im + OH^- \qquad \Delta G = 1.4 \text{ kcal/mol}$$

$$Im + H_2O \rightarrow ImH^+ + OH^- \qquad \Delta = 12.2 \text{ kcal/mol}$$

It is not surprising to see that these energies are substantially different from those in Figure 4 for processes III → IV, IV → VI, and III → V, respectively. As already noted, there are two major reasons for this: (1) the strong donor–acceptor electrostatic potential at fixed, short distances, which significantly modifies the reaction energetics; and (2) the necessity for use of extended basis set and high-level-correlated methods for accurately reproducing proton affinities. Such computations would be too costly and are beyond the scope of the present study.

As Figure 4 indicates, deprotonation of the water molecule is a difficult step. Note that the activation energy may be lowered by changing the water molecule by a serine residue (or by a CH_3OH unit). Such an effect would be present in all steps involving proton transfer to imidazole, with structures V and VI being notably stabilized. Note also that, in enzymes, the deprotonation of the serine residue is favored by the nucleophilic attack of the forming RO^- anion to the substrate.

Some additional comments on Figure 4 can be made by comparison of elementary process energetics. The activation barrier for deprotonation of the water molecule is lower when it is preceded by proton transfer from imidazole to formate (i.e., in the CR2 mechanism). Conversely, proton transfer from imidazole to formate is made with small barriers. This is especially true for the product interconversion process V → VI, because the donating species is protonated imidazole. The activation barrier, in this case, is 4.5 kcal/mol, which may be compared with 9.7 kcal/mol for III → IV in the first step of the stepwise CR2 process. Also, it is noteworthy that structure VI is 4.7 kcal/mol more stable than structure V; that is, in a polar environment, these calculations predict that the system formed after proton transfer from water to imidazole may be stabilized by a second proton transfer from imidazole to formate. Protonation of imidazole does not produce spontaneous proton

transfer to carboxylate, but the latter process is quite simple because it requires a low energy barrier (4.5 kcal/mol, see earlier). Analysis of the SCRF computations shows that polar medium slightly favors VI over V (The electrostatic interaction with environment amounts about −97 and −95 kcal/mol for VI and V, respectively; in addition, note that the electrostatic interaction energy for III and IV is much smaller, about 59 kcal/mol, which explains why V and VI are not stable in gas phase).

Role of Environment Fluctuations

Because proton transfer processes involve a substantial charge reorganization of the chemical system, the equilibrated environment configurations for the reactants, transition state, and products may exhibit large differences in polarization. Thus, if reaction time is significantly shorter than the relaxation time of the environment, the latter cannot follow the reactive event and nonequilibrium effects arise.[40] The polarization of the surrounding solvent or protein has different components, which in many cases may be separated into a noninertial polarization term, associated with electronic polarizability, and an inertial term, associated with atomic (translational + vibrational) and rotational motions in the molecular environment. The inertial polarization is characterized by a long relaxation time as compared with the reaction time and may be reasonably assumed to be frozen during proton transfer. On the other hand, noninertial polarization is fast and the corresponding component may be assumed to equilibrate instantaneously the modifications of the chemical system charge distribution. According to these assertions, the relevant energy surface for the proton transfer is not the equilibrium one, but rather that obtained for the current configuration of the environment. Such a configuration is continuously fluctuating, and the reaction occurs when the energy barrier displays a minimum value.[26a, 27a]

Protein fluctuations play an important role in enzymatic reaction dynamics[41] as MD simulations by Warshel and coworkers[26a, 27, 42] have demonstrated. In particular, in the study of the catalytic reaction of lysozyme, Warshel[27a] showed that protein fluctuations are intimately related to reaction kinetics. The barrier for proton transfer fluctuates as a function of the structural fluctuation of the protein. For some protein fluctuations (in ref. 27a referred to as ''catalytic fluctuations'') the transition state is stabilized and proton transfer is favored. Obviously, the reaction rate must be related to the probability of reaching such fluctuations, which depends on several factors, and in principle can be different for a solvent or a protein environment. However, Warshel and coworkers found that dynamic effects are not very different in enzyme and solvent reactions.[26a, 27]

Although MD is, in principle, the appropriate technique to study dynamic effects of the environment in chemical reactions, a qualitative study can be done by using simple dielectric continuum models, such as the one developed by our group.[43] In our model, a fluctuation of the environment is represented by changes in the reaction field around its equilibrium value. The reaction field has two components corresponding to the noninertial and inertial polarization terms. The former is always in equilibrium with the solute charge and is evaluated using the infinite frequency dielectric constant. The inertial term may take arbitrary values, but in practice it is useful to consider configurations in equilibrium with the chemical system at different points along the reaction coordinate. The advantage of such an approach is that the solute (or the active site) can be described quantum mechanically at any desired level of accuracy. Our aim here was to undertake such a study for proton transfer in the imidazole–formate–water system in aqueous solution. MD simulations of proton transfer reactions using combined quantum mechanics and molecular mechanics potentials are also feasible,[26c] and investigation of dynamic solvent effects on model triads will be reported in due course.

We take the example of the process III → IV as an illustration. The internal coordinate constraints are the same as those indicated in the previous section. Two different cases are considered in which the frozen inertial polarization is assumed to be that in equilibrium with the reactants (case a) or the transition state (case b). This corresponds to two different physical situations. In case a, we assume initial solute–solvent equilibrium; in case b, we assume that the reactant–solvent system has reached a nonequilibrium configuration through a convenient fluctuation of the environment. The noninertial part of the solvent polarization is always relaxed. In such conditions, we scan the NH distance and we look at the variation of the total energy of the system in the dielectric environment.

The results are plotted in Figure 5. It is shown that the curve corresponding to case a presents a deep energy well for reactant III and a very shallow energy minimum for product IV. This means that only reactant III is stable in such conditions and that proton transfer is not possible. Conversely, fluctuation of the environment to a TS-like configuration, case b, leads to a double-well energy curve that presents an energy barrier of about 5 kcal/mol (this barrier is almost half the equilibrium barrier for the same system, see Fig. 4). The absence of a product minima in case a is not surprising if one bears in mind that the barrier for inverse proton transfer (III → IV) in the equilibrium surface is rather small (3.2 kcal/mol, see Table IV). Nonequilibrium solvation adds always a destabilizating energy contribution whose magnitude depends on the difference between the hypothetical equilibrium and actual environmental polarization. If we examine the case a curve, this difference increases from the reactants (which are in equilibrium) to the product, because the polarity of the chemical system is reversed. Accordingly, the destabilizing effect is larger for the product than for the TS and flattens the energy surface in the product side.

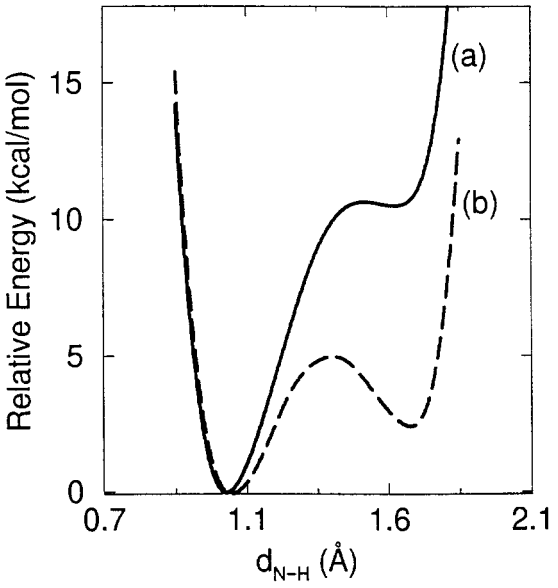

FIGURE 5. Energy profiles for proton transfer from imidazole to formate III → IV in a polar dielectric environment under nonequilibrium conditions (i.e., for a frozen solvent inertial polarization term). (a) Frozen inertial polarization with the reactant-like configuration. (b) Frozen inertial polarization with the TS-like configuration reached by fluctuation.

In a recent study of model proton transfer processes in aqueous solution using MD simulations and sophisticated quantum/classical potentials,[26c] it has been shown that TS-like solvent fluctuations are relatively rare. Nevertheless, solvent fluctuations, with frequency in the 10–30 ps^{-1} range, may contribute as much as 50% to the instantaneous electric field felt by the chemical system. These fluctuations are related to equilibrium solvation of a solute structure lying halfway between the reactant and the TS. Assuming that the probability of solvent fluctuations is similar in our case, the proton-transfer energy profile for the most probable ''catalytic'' solvent fluctuations would be a curve lying between case a and b in Figure 5.

We have not computed nonequilibrium energy paths for the other processes. However, some qualitative trends may be inferred on the basis of the results presented. Let us consider the single-proton SP mechanism III → V. In this case, we note that the inverse barrier III ← V is very low (3.4 kcal/mol, see Fig. 4). Hence, the role of environmental fluctuations is expected to be as important as in the previous study: without them, the energy curve is of single-well type and proton transfer is not possible. If we consider the concerted double-proton-transfer CR1 mechanism III → VI, it can be seen that the energy difference between the minima (reactant or product) and the transition state is substantial, so that the nonequilibrium effect may play a role, yet environmental fluctuations are not required to create a product energy well. Finally, for the CR2 mechanism III → IV → VI, nonequilibrium effects are more difficult to predict because two consecutive process are involved and both fluctuations and relaxation of the environment will result in complex nonequilibrium effects.

Conclusions

Our first conclusion deals with the proton-transfer mechanism in the formate–imidazole complex, which has been studied in gas phase and in solution. In solution, the process is not favored kinetically (although it is favored thermodynamically). Conversely, when a water molecule is hydrogen bonded to the N atom of the imidazole ring, the proton transfer is favored. This result illustrates that specific interactions may modify the conventional belief that, in $AH \cdots B^- \rightarrow A^- \cdots HB$ processes, solvation energy always tends to increase the activation energy barriers.

We have also investigated double-proton-transfer mechanisms in the model triad formate–imidazole–water complex. The main conclusion is that the stepwise charge-relay (CR2) and single-proton (SP) mechanisms appear to have similar energetics, whereas the concerted charge-relay mechanism requires greater activation energy. Moreover, the existence of a transition structure may be questioned for the latter mechanism. The preference of a CR2 or SP mechanism will depend on the actual conditions of the process and one may expect that, by slightly changing such conditions, the mechanism also changes. For instance, in enzymatic catalysis, the mechanism may be quite sensitive to the proteic environment and conclusions reached experimentally for model systems do not necessarily apply for real enzymes *in vivo*.

Finally, we have demonstrated that nonequilibrium effects have to be taken into account for a deep understanding of the reactions. Similar conclusions have already been reported in the literature for both reactions in solution and enzyme-catalyzed reactions. Indeed, proton transfer is a very fast process, so that the environment cannot relax anywhere along the reaction coordinate. TS-like fluctuations of the environment stabilize the product and decrease the activation barrier, whereas reactant-like solvent configurations make the reaction basically nonfeasible. Differences between solution and protein fluctuations have not been computed here, but have been shown to be rather small in previous works.[27] Hence, although fluctuations are important for explaining reaction dynamics, the catalytic role of enzymes is not necessarily related to them.

References

1. (a) J. H. Wang, *Science*, **161**, 328 (1968); (b) L. Polgar and M. L. Bender, *Proc. Natl. Acad. Sci. USA*, **64**, 1335 (1969).
2. (a) D. M. Blow, J. J. Birktoft, and B. S. Hartley, *Nature*, **221**, 337 (1969); (b) M. W. Hunkapiller, S. H. Smallcombe, D. R. Whitaker, and J. H. Richards, *Biochemistry*, **12**, 4732 (1973); (c) R. E. Koeppe and R. M. Stroud, *Biochemistry*, **15**, 3450 (1976).
3. (a) G. Robillard and R. G. Shulman, *J. Mol. Biol.*, **86**, 541 (1974); (b) J. L. Markley and M. A. Porubcan, *J. Mol. Biol.*, **102**, 487 (1976); (c) W. W. Bachovchin and J. D. Roberts, *J. Am. Chem. Soc.*, **100**, 8041 (1978); (d) A. A. Kossiakoff and S. A. Spencer, *Nature*, **288**, 414 (1980); (e) A. A. Kossiakoff and S. A. Spencer, *Biochemistry*, **20**, 6462 (1981).
4. W. W. Bachovchin, *Biochemistry*, **25**, 7751 (1986).
5. S. O. Smith, S. Farr-Jones, R. G. Griffin, and W. W. Bachovchin, *Science*, **244**, 961 (1989).
6. M. E. McGrath, J. R. Vásquez, C. S. Craik, A. S. Yang, B. Honig, and R. J. Fletterick, *Biochemistry*, **31**, 3059 (1992).
7. N. Wellner and G. Zundel, *J. Mol. Struct.*, **317**, 249 (1994).
8. W. L. Mock and D. C. Y. Chua, *J. Chem. Soc., Perkin Trans.*, **2**, 2069 (1995).
9. T. K. Chang, Y. Chiang, H.-X. Guo, A. J. Kresge, L. Mathew, M. F. Powell, and J. A. Wells, *J. Am. Chem. Soc.*, **118**, 8802 (1996).
10. (a) P. A. Frey, S. A. Whitt, and J. B. Tobin, *Science*, **264**, 1927 (1994); (b) S. B. Tobin, S. A. Whitt, C. S. Cassidy, and P. A. Frey, *Biochemistry*, **34**, 6919 (1995); (c) C. S. Cassidy, J. Lin, and P. A. Frey, *Biochemistry*, **36**, 4576 (1997); (d) E. L. Ash, J. L. Sudmeier, E. C. De Fabo, and W. W. Bachovchin, *Science*, **278**, 1128 (1997).
11. (a) H. Umeyama, A. Imamura, C. Nagata, and M. Hanano, *J. Theor. Biol.*, **41**, 485 (1973); (b) S. Scheiner, D. A. Kleier, and W. N. Lipscomb, *Proc. Natl. Acad. Sci. USA*, **72**, 2606 (1975); (c) S. Scheiner and W. N. Lipscomb, *Proc. Natl. Acad. Sci. USA*, **73**, 432 (1976).
12. M. J. S. Dewar and D. M. Storch, *Proc. Natl. Acad. Sci. USA*, **82**, 2225 (1985).
13. (a) D. M. Hayes and P. A. Kollman, In *Catalysis in Chemistry and Biochemistry: Theory and Experiment*, B. Pullman, Ed., D. Reidel, Boston, 1979, p. 77; (b) P. A. Kollman and D. M. Hayes, *J. Am. Chem. Soc.*, **103**, 2955 (1981); (c) H. Umeyama and S. Nakagawa, *Chem. Pharm. Bull.*, **30**, 2252 (1982); (d) H. Umeyama and S. Nakagawa, *J. Theor. Biol.*, **99**, 759 (1982).
14. (a) S. Nakagawa and H. Umeyama, *Bioorg. Chem.*, **11**, 322 (1982); (b) S. Nakagawa and H. Umeyama, *J. Mol. Biol.*, **179**, 103 (1984); (c) H. Umeyama, S. Hirono, and S. Nakagawa, *Proc. Natl. Acad. Sci. USA*, **81**, 6266 (1984); (d) E. Longo, F. M. L. G. Stamato, R. Ferreira, and O. Tapia, *J. Theor. Biol.*, **112**, 783 (1985).
15. (a) A. Warshel and S. Russell, *J. Am. Chem. Soc.*, **108**, 6579 (1986); (b) A. Warshel, G. Náray-Szabó, F. Sussman, and J.-K. Hwang, *Biochemistry*, **28**, 3629 (1989).
16. F. M. L. G. Stamato and O. Tapia, *Int. J. Quant. Chem.*, **33**, 187 (1988).
17. V. Daggett, S. Schröder, and P. Kollman, *J. Am. Chem. Soc.*, **113**, 8926 (1991).
18. S. Nakagawa, H. A. Yu, M. Karplus, and H. Umeyama, *Proteins*, **16**, 172 (1993).
19. W. Brandt, O. Ludwig, I. Thondorf, and A. Barth, *Eur. J. Biochem.*, **236**, 109 (1996).
20. (a) G. Dive, D. Dehareng, and D. Peeters, *Int. J. Quant. Chem.*, **58**, 85 (1996); (b) J. G. Ángyán, G. Kramer, P. Nagy, P. R. Surján, and G. Náray-Szabó, In *Theoretical Biochemistry and Molecular Biophysics*, D. L. Beveridge and R. Lavery, Eds., Adenine Press, New York, 1990, p. 153; (c) J. G. Ángyán and G. Náray-Szabó, *J. Theor. Biol.*, **103**, 349 (1983).
21. (a) M. Komiyama and M. L. Bender, *Bioorg. Chem.*, **6**, 13 (1977); (b) M. Komiyama, M. L. Bender, M. Utaka, and A. Takeda, *Proc. Natl. Acad. Sci. USA*, **74**, 2634 (1977); (c) K. S. Venkatasubban and R. L. Schowen, *CRC Crit. Rev. Biochem.*, **17**, 1 (1984); (d) R. L. Stein, A. M. Strimpler, H. Hori, and J. C. Powers, *Biochemistry*, **26**, 1305 (1987); (e) J. D. Scholten, J. L. Hogg, and F. M. Raushel, *J. Am. Chem. Soc.*, **110**, 8246 (1988).
22. (a) G. A. Rogers and T. C. Bruice, *J. Am. Chem. Soc.*, **96**, 2473 (1974); (b) S. C. Zimmerman, J. S. Korthals, and K. D. Cramer, *Tetrahedron*, **47**, 2649 (1991).

23. A. R. Fersht, *Enzyme Structure and Mechanism* (2nd ed.), W.H. Freeman & Co., New York, 1985.
24. (a) W. W. Cleland, *Biochemistry*, **31**, 317 (1992); (b) J. A. Gerit and P. G. Gassman, *Biochemistry*, **32**, 11943 (1993); (c) J. A. Gerit, *J. Am. Chem. Soc.*, **115**, 11552 (1993); (d) W. W. Cleland and M. M. Kreevoy, *Science*, **264**, 1887 (1994); (e) W. W. Cleland and M. M. Kreevoy, *Science*, **269**, 104 (1995); (f) P. A. Frey, *Science*, **269**, 104 (1995); (g) A. Warshel, A. Papazyan, and P. A. Kollman, *Science*, **269**, 102 (1995); (h) S. Scheiner and T. Kar, *J. Am. Chem. Soc.*, **117**, 6970 (1995); (i) G. Alagona, C. Ghio, and P. A. Kollman, *J. Am. Chem. Soc.*, **117**, 9855 (1995); (j) S. Shan, S. Loh, and D. Herschlag, *Science*, **272**, 97 (1996); (k) Y. Kato, L. M. Toledo, and J. Jr. Rebek, *J. Am. Chem. Soc.*, **118**, 8575 (1996); (l) A. Warshel and A. Papayzan, *Proc. Natl. Acad. Sci. USA*, 96, 13665 (1996); (m) M. García-Viloca, A. González-Lafont, and J. M. Lluch, *J. Am. Chem. Soc.*, **119**, 1081 (1997); (n) M. García-Viloca, A. González-Lafont, and J. M. Lluch, *J. Phys. Chem. A*, **101**, 3880 (1997); (o) Y. Pan and M. A. McAllister, *J. Am. Chem. Soc.*, **119**, 7561 (1997).
25. (a) A. Warshel and M. Levitt, *J. Mol. Biol.*, **103**, 227 (1976); (b) P. D. Lyne, A. J. Mulholland, and W. G. Richards, *J. Am. Chem. Soc.*, **117**, 11345 (1995); (c) G. Monard, M. Loos, V. Théry, K. Baka, and J.-L. Rivail, *Int. J. Quant. Chem.*, **58**, 153 (1996); (d) H. Liu, F. Müller-Plathe, and W. F. van Gunsteren, *J. Mol. Biol.*, **261**, 454 (1996); (e) M. J. Harrison, N. A. Burton, I. H. Hillier, and I. R. Gould, *Chem. Comm.*, **2769** (1996); (f) A. J. Mulholland and W. G. Richards, *Proteins*, **27**, 9 (1997).
26. (a) A. Warshel, *Computer Modeling of Chemical Reactions in Enzymes and Solutions*, John Wiley & Sons, New York, 1991; (b) J. J. Timoneda and J. T. Hynes, *J. Phys. Chem.*, **95**, 10431 (1991); (c) I. Tuñón, M. T. C. Martins-Costa, C. Millot, and M. F. Ruiz-López, *J. Chem. Phys.*, **106**, 3633 (1997).
27. (a) A. Warshel, *Proc. Natl. Acad. Sci. USA*, **81**, 444 (1984); (b) A. Warshel, F. Sussman and J.-K. Hwang, *J. Mol. Biol.*, **201**, 139 (1988).
28. (a) D. Wei and D. R. Salahub, *J. Chem. Phys.*, **101**, 7633 (1994); (b) Z. Latajka, Y. Bouteiller, and S. Scheiner, *Chem. Phys. Lett.*, **234**, 159 (1995); (c) B. S. Jursic, *Chem. Phys. Lett.*, **244**, 263 (1995); (d) J. W. Andzelm, D. T. Nguyen, R. Eggenberger, D. R. Salahub, and A. T. Hagler, *Computers Chem.*, **19**, 145 (1995); (e) H. Chojnacki, J. Andzelm, D. T. Nguyen, and W. A. Sokalski, *Computers Chem.*, **19**, 181 (1995); (f) Q. Zhang, R. Bell, and T. N. Truong, *J. Phys. Chem.*, **99**, 592 (1995); (g) G. J. Tawa, R. L. Martin, L. R. Pratt, and T. V. Russo, *J. Phys. Chem.*, **100**, 1515 (1996); (h) W.-G. Han and S. Suhai, *J. Phys. Chem.*, **100**, 3942 (1996).
29. (a) J. C. Slater, *Quantum Theory of Molecules and Solids. Vol. 4: The Self-Consistent Field for Molecules and Solids*, McGraw-Hill, New York, 1974; (b) A. D. Becke, *Phys. Rev. A*, **38**, 3098 (1988).
30. C. Lee, W. Yang, and R. G. Parr, *Phys. Rev. B*, **37**, 785 (1988).
31. W. J. Hehre, R. Ditchfield, and J. A. Pople, *J. Chem. Phys.*, **56**, 2257 (1972). The usual * notation holds for polarization functions on first-row atoms as proposed in: P. C. Hariharan and J. A. Pople, *Theoret. Chim. Acta*, **28**, 213 (1973).
32. (a) V. Dillet, D. Rinaldi, J. G. Ángyán, and J. L. Rivail *Chem. Phys. Lett.*, **202**, 18 (1993); (b) M. F. Ruiz-López, F. Bohr, M. T. C. Martins-Costa, and D. Rinaldi, *Chem. Phys. Lett.*, **221**, 109 (1994); (c) J. L. Rivail and D. Rinaldi, In *Computational Chemistry. Reviews of Current Trends, Vol. 1*, J. Leszczynski, Ed.; World Scientific Pub. 1996, p. 139.
33. M. J. Frisch, G. W. Trucks, H. B. Schlegel, P. M. W. Gill, B. G. Johnson, M. A. Robb, J. R. Cheeseman, T. Keith, G. A. Petersson, J. A. Montgomery, K. Raghavachari, M. A. Al-Laham, V. G. Zakrzewski, J. V. Ortiz, J. B. Foresman, C. Y. Peng, P. Y. Ayala, W. Chen, M. W. Wong, J. L. Andres, E. S. Replogle, R. Gomperts, R. L. Martin, D. J. Fox, J. S. Binkley, D. J. Defrees, J. Baker, J. P. Stewart, M. Head-Gordon, C. Gonzalez, and J. A. Pople, Gaussian-94, Revision B.3, Gaussian, Inc., Pittsburgh, PA, 1995.
34. R. R. Pappalardo and D. Rinaldi, SCRFPAC, QCPE No. 622, Indiana University, Bloomington, IN, 1992; D. Rinaldi, updated version of SCRFPAC for Gaussian-94, personal communication.
35. H. B. Schlegel, *J. Comput. Chem.*, **3**, 214 (1982).
36. I. A. Koppel, U. H. Molder, and V. Palm, *Org. Reactivity*, **22**, 77 (1985).
37. (a) S. G. Lias, J. E. Liebman, and R. D. Levin, *J. Phys. Chem. Ref. Data*, **13**, 695 (1984); (b) S. G. Lias, J. E. Bartmess, J. L. Holmes, R. D. Levin, J. F. Liebman, and W. G. Mallard, *J. Phys. Chem. Ref. Data*, **17**(Suppl. 1) (1988).
38. (a) G.-S. Li, M. F. Ruiz-López, M.-S. Zhang, and B. Maigret, *J. Mol. Struct., Theochem.*, **422**, 197 (1998); (b) G.-S. Li, M. F. Ruiz-López, and B. Maigret, *J. Phys. Chem. A*, **101**, 7885 (1997).
39. S. Scheiner and M. Yi, *J. Phys. Chem.*, **100**, 9235 (1996).
40. Some basic concepts have been developed in: H. A. Kramers, *Physica*, **7**, 284 (1940); R. A. Marcus, *J. Chem. Phys.*, **24**, 966 (1956); J. L. Kurz and L. C. Kurz, *J. Am. Chem. Soc.*, **94**, 4451 (1972); G. van der Zwan and J. T. Hynes, *J. Chem. Phys.*, **76**, 4174 (1983).
41. For a review see: G. R. Welch, B. Somogyi, and S. Damjanovich, *Prog. Biophys. Molec. Biol.*, **39**, 109 (1982);
42. A. Warshel, Z. T. Chu, and W. W. Parson, *Science*, **246**, 112 (1989).
43. M. F. Ruiz-López, D. Rinaldi, and J. Bertrán, *J. Chem. Phys.*, **103**, 9249 (1995).